$$y = \frac{P_1}{1 + \exp[P_2(x - P_3)]} + P_4 \quad (1)$$

where x and y represent the input and the output, respectively. P_1 denotes the response range (i.e., the difference between the maximum and minimum values of y), P_2 is the coefficient of gain, P_3 is the midpoint of the logistic function on the input axis, and P_4 is the minimum value of y. The maximum gain (G_{max}) is calculated from $-P_1P_2/4$ at $x = P_3$. The parameter values were calculated by an iterative nonlinear least-squares regression known as the downhill simplex method.

Statistical Analysis

All data are presented as means ± SD. Differences were considered to be significant when $P < 0.05$. In *protocols 1-1, 2, 3,* and *4*, the effects of electroacupuncture on AP and SNA at different time intervals were evaluated by one-way ANOVA. The Dunnett's test was used for multiple comparisons. In *protocols 1-2* and *1-3*, the effects of electroacupuncture on the four parameters of the logistic functions relating to the neural and peripheral arcs, as well as on the closed-loop operating point, were examined by using a paired *t*-test.

RESULTS

Figure 1*A* (*protocol 1-1*) shows a typical time series of AP and SNA in response to Zusanli-Xiajuxu electroacupuncture with intact cardiovascular reflexes. AP and SNA were reduced immediately after beginning electroacupuncture, and these remained reduced during 8-min electroacupuncture. Figure 1*B* illustrates the group-averaged AP and SNA in response to electroacupuncture. AP and SNA for baseline were unchanged by acupuncture insertion alone, while these values for 8-min electroacupuncture remained decreased from baseline. These values returned to baseline level after the cessation of electroacupuncture.

Figure 2 (*protocol 1-2*) shows a typical AP and SNA response to the increments in CSP in the control (Fig. 2, *left*) and electroacupuncture (Fig. 2, *right*) trials. A stepwise increase in CSP decreased SNA and AP in both trials. In the electroacupuncture trial, the AP and SNA response ranges to CSP were attenuated compared with the control trial.

Figure 3, *A* and *B* (*protocol 1-2*), shows the averaged baroreflex neural and peripheral arcs obtained in control and electroacupuncture trials. The neural arc showed a sigmoidal relationship between CSP and SNA. In the neural arc, the response range of SNA (P_1) and midpoint of the operating range (P_3) were significantly decreased by electroacupuncture (Table 1). The coefficient of gain (P_2), the minimum value of SNA (P_4), and G_{max} did not differ between the two trials (Table 1). As a result, the maximum value of SNA, calculated from $P_1 + P_4$, was significantly decreased by electroacupuncture from 162 ± 31 to 130 ± 29 au ($P < 0.005$). The peripheral arc showed a more linear relationship between SNA and AP than the neural arc. In the peripheral arc, electroacupuncture did not affect any of the four parameters or G_{max} (Table 1 and Fig. 3*B*). The operating point determined by the intersection of the neural and peripheral arcs was moved toward lower AP and SNA (from *point a* to *point b*) by electroacupuncture (Fig. 3*C* and Table 1).

Figure 4 (*protocol 1-3*) shows the averaged baroreflex neural (Fig. 4*A*) and peripheral arcs (Fig. 4*B*) in control and electroacupuncture trials with severance of the peroneal nerve innervating the tibialis anterior muscle. Two arcs obtained in both trials were nearly superimposable. The four parameters and G_{max} in the neural and peripheral arcs and operating point were

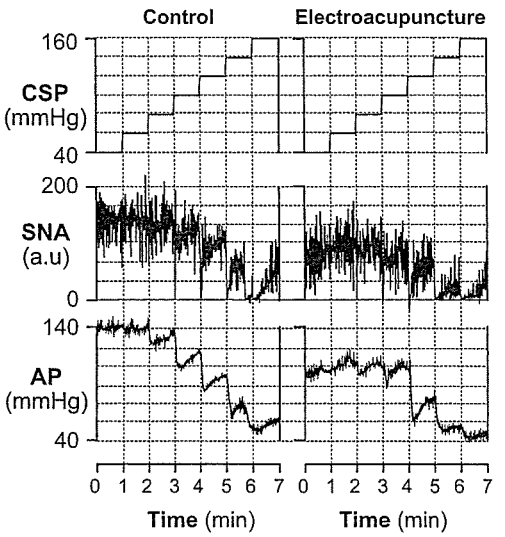

Fig. 2. Typical time series of intra-carotid sinus pressure (CSP), AP, and SNA in control (*left*) and electroacupuncture trials (*right*) in *protocol 1-2*. SNA and AP decreased in response to increments in CSP in both of the two trials. The response ranges of AP and SNA to CSP were lower in electroacupuncture than in controls.

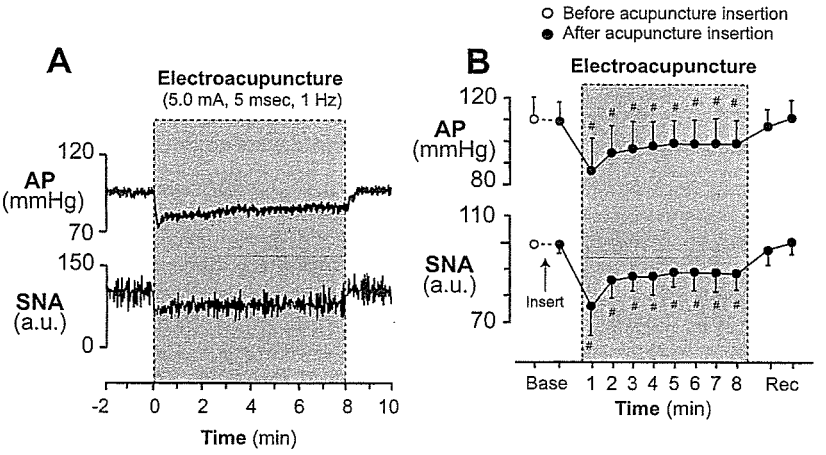

Fig. 1. Typical time series of arterial pressure (AP) and sympathetic nerve activity (SNA) during 8 min of 1-Hz electroacupuncture (*A*) and the averaged ($n = 6$) AP and SNA (*B*) in *protocol 1-1*. Data include periods of baseline (Base, 1 min), electroacupuncture (8 min), and recovery (Rec, 1 min). Each data point represents average values over 1 min. #$P < 0.05$: significantly different from baseline after acupuncture insertion. au, Arbitrary units.

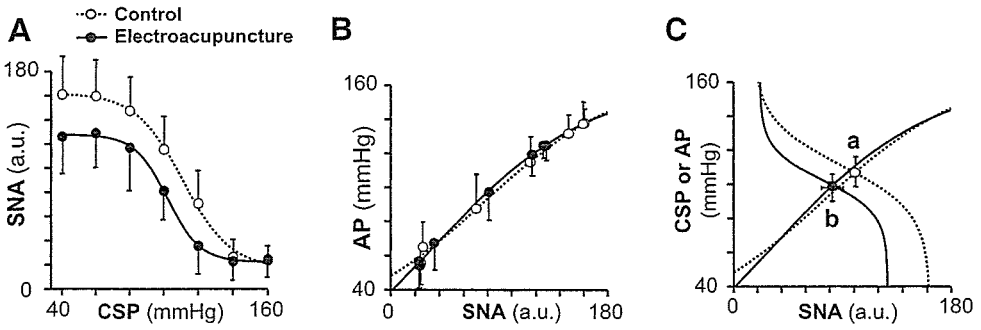

Fig. 3. Averaged (n = 8) baroreflex neural arc (*A*), peripheral arc (*B*), and baroreflex equilibrium diagram (*C*) obtained in 8 rabbits in control (○) and electroacupuncture (●) trials in *protocol 1-2*. Electroacupuncture shifted the neural arc to lower SNA (*A*), but it did not change the peripheral arc (*B*). The shift in neural arc reduced AP and SNA by 9 ± 3 mmHg and 20 ± 10 au (from *point a* to *point b*) at the operating point (*C*).

not affected by electroacupuncture when the peroneal nerve was denervated (Table 2 and Fig. 4*C*).

Figure 5 (*protocol 2*) shows the changes in AP and SNA during nonacupuncture (without acupuncture), sham acupuncture [nonelectrical acupuncture at Zusanli-Xiajuxu (St 36–39)], control acupuncture [nonelectrical acupuncture at Guangming-Xuanzhong (Gb 37–39)] and control electroacupuncture (electrical acupuncture at Gb 37–39) trials. AP and SNA did not change in these trials.

Figure 6, *A* and *B* (*protocol 3*), shows a typical time series and the averaged data, respectively, of AP and SNA in response to long-term Zusanli-Xiajuxu electroacupuncture. AP and SNA decreased immediately after electroacupuncture was started and remained reduced during 30-min electroacupuncture. In addition, AP and SNA returned to the preelectroacupuncture baseline levels immediately after cessation of electroacupuncture.

Figure 7, *A* and *B* (*protocol 4*), shows a typical time series and the averaged data, respectively, of AP and SNA during Zusanli-Xiajuxu electroacupuncture with the pulse duration increasing from 0.1 to 5 ms. Although increasing the pulse duration from 0.1 to 1 ms did not change AP and SNA, pulse durations of 2.5 ms and higher decreased SNA while pulse durations of 5 and 10 ms decreased AP.

Table 1. *Effect of electroacupuncture on the operating point of baroreflex and on the 4 parameters of logistic functions approximating neural and peripheral baroreflex arcs*

	Control	Electroacupuncture
Operating point		
Arterial pressure, mmHg	108.4±8.7	98.8±7.9†
Sympathetic nerve activity, au	99.8±4.1	80.0±8.9†
Neural arc		
P_1, au	144.0±35.0	112.6±9.2†
P_2, au/mmHg	0.08±0.03	0.09±0.09
P_3, mmHg	111.4±6.5	103.3±10.0*
P_4, au	17.5±6.1	17.4±8.7
G_{max}, au/mmHg	−2.94±0.91	−2.58±1.27
Peripheral arc		
P_1, mmHg	129.6±20.5	125.9±19.5
P_2, au/mmHg	−0.03±0.01	−0.03±0.01
P_3, au	80.6±23.2	71.7±17.1
P_4, mmHg	29.9±16.3	29.5±12.1
G_{max}, mmHg/au	0.74±0.10	0.84±0.18

Values are means ± SD (n = 8). G_{max}, maximum gain. See *Data Analysis* for definition of 4 parameters of logistic function. au, Arbitrary units. *P < 0.05 and †P < 0.005 vs. control.

DISCUSSION

The major new finding of the present study was that electroacupuncture at Zusanli resets the arterial baroreflex neural arc to lower SNA but does not significantly affect the baroreflex peripheral arc. As a result, the operating point determined by the intersection of the neural and peripheral arcs was moved toward lower SNA and AP by electroacupuncture. To the best of our knowledge, this is the first study delineating the effects of short-term electroacupuncture on the arterial baroreflex over an entire operating range.

Effects of Electroacupuncture on the Arterial Baroreflex (Protocol 1)

The arterial baroreflex system is one of the most important negative-feedback systems that stabilize AP against exogenous disturbances. When AP is decreased by exogenous perturbation such as blood loss, the reduction in AP is sensed by the arterial baroreceptors. SNA is then increased by the arterial baroreflex to buffer the reduction in AP. In such circumstances, SNA and AP change reciprocally. On the other hand, when SNA is changed by an exogenous perturbation such as emotional stress, SNA and AP change in parallel. In *protocol 1-1*, electroacupuncture decreased both SNA and AP, indicating that electroacupuncture introduced exogenous perturbation to decrease SNA with a resultant reduction in AP. Although the net effect of electroacupuncture is to decrease SNA, the perturbation of AP cannot be excluded. For example, because electroacupuncture also twitched the hindlimb muscles, electroacupuncture might have perturbed AP via changes in vascular resistance and/or venous return through muscle pump function. Therefore, to quantify the contribution of both perturbations on SNA and on AP, we performed *protocol 1-2*. Perturbation of AP is most easily detected by comparing AP at the same SNA level with and without electroacupuncture.

In *protocol 1-2*, we performed a baroreflex open-loop experiment and identified the static characteristics of the neural and peripheral arcs over a wide operating range. As expected, electroacupuncture shifted the neural arc toward lower SNA and decreased maximum SNA to ~80% of control (Fig. 3*A*). This shift is not due to reduced perfusion to the medulla by AP reduction during electroacupuncture because the AP was decreased by ~10 mmHg and would not induce cerebral ischemia. In contrast, electroacupuncture had little effect on the peripheral arc (Fig. 3*B*). In other words, AP with and without electroacupuncture did not differ significantly at any of the SNA levels. Therefore, changes in AP observed in *protocol 1-1*

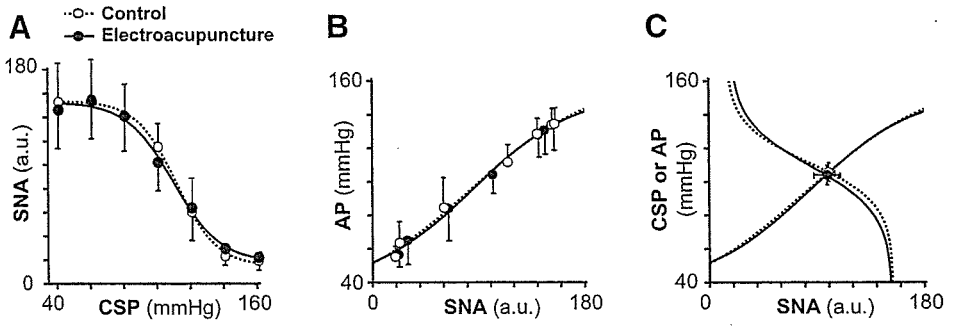

Fig. 4. Averaged (n = 6) baroreflex neural arc (A), peripheral arc (B), and baroreflex equilibrium diagrams (C) obtained in 6 rabbits in control (○) and electroacupuncture (●) trials with peroneal denervation in *protocol 1-3*. The baroreflex neural arc, peripheral arc, and the operating point were not influenced by electroacupuncture after peroneal denervation.

were attributable exclusively to perturbation of SNA and not to possible perturbation effects of electroacupuncture on AP.

The neural and peripheral arcs were combined to yield a baroreflex equilibrium diagram (Fig. 3*C*). The closed-loop operating point, determined by the intersection of the neural and peripheral arcs, moved from *point a* to *point b* during electroacupuncture. Despite a significant shift in the closed-loop operating point, neither the neural nor peripheral arc gain was altered significantly (Table 1). The fact that the baroreflex gain was maintained during electroacupuncture suggests the possible application of electroacupuncture to the treatment of cardiovascular diseases with sympathetic hyperactivity. However, the preservation of the arterial baroreflex gain in the present experimental settings may rely on normal peripheral arc characteristics. Cardiovascular diseases such as heart failure may decrease the peripheral arc gain to a variable extent due to impaired pump function. Whether the arterial baroreflex function during electroacupuncture can be maintained in cardiovascular diseases awaits future study.

Mechanisms for the Cardiovascular Inhibitory Effects of Electroacupuncture (Protocol 1)

The resetting in the baroreflex neural arc during electroacupuncture was mediated by a somatosympathetic reflex arising from the stimulated hindlimb, as evidenced by the fact that peroneal denervation abolished the resetting (Table 2 and Fig. 4). This result was consistent with an earlier study (27) showing that depressor and sympathoinhibitory responses during acupuncture were abolished by sciatic and femoral denervation. The existence of a somatosympathetic reflex is also supported by the fact that electrical stimulation of somatic afferents reduced AP (7–9). Legramante et al. (14) showed that rapidly conducting group III somatic afferent activation can evoke AP reduction during 1-Hz electrical stimulation of the tibial nerve. In contrast, high-frequency stimulation of the somatic afferent evokes AP elevation. Passive muscle stretching, which is considered to activate group III somatic afferent fibers, shifts the baroreflex neural arc toward higher SNA, resulting in an increase in the closed-loop operating point (41). The mechanism of two opposing influences of somatic afferent activation depending on the stimulation frequency is not fully understood.

Table 2. *Effect of electroacupuncture with peroneal denervation on the operating point of baroreflex and on the 4 parameters of logistic functions approximating neural and peripheral baroreflex arcs*

	Control	Electroacupuncture
Operating point		
Arterial pressure, mmHg	105.7±5.7	104.1±5.6
Sympathetic nerve activity, au	99.8±5.1	98.3±11.1
Neural arc		
P_1, au	138.3±42.4	136.3±38.6
P_2, au/mmHg	0.11±0.03	0.08±0.03
P_3, mmHg	112.7±10.2	111.5±10.6
P_4, au	14.9±8.7	15.7±7.4
G_{max}, au/mmHg	−3.27±1.15	−2.84±1.12
Peripheral arc		
P_1, mmHg	144.1±35.5	140.5±34.4
P_2, au/mmHg	−0.02±0.002	−0.02±0.004
P_3, au	82.0±34.0	78.8±32.0
P_4, mmHg	26.1±8.1	25.5±5.3
G_{max}, mmHg/au	0.69±0.13	0.72±0.21

Values are means ± SD (n = 6). See *Data Analysis* for definition of 4 parameters of logistic function.

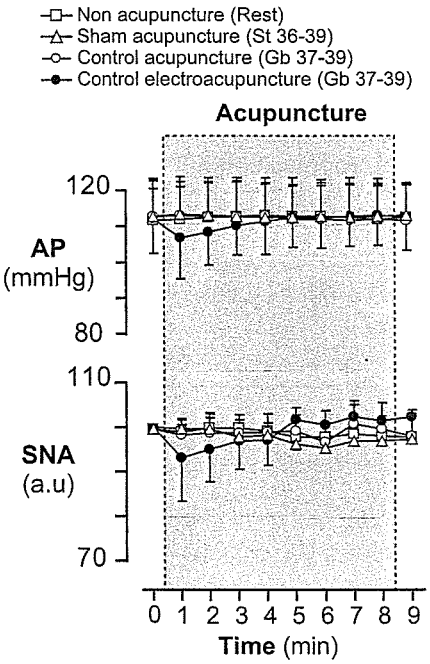

Fig. 5. Averaged (n = 6) AP (*top*) and SNA (*bottom*) in nonacupuncture (condition without acupuncture, □), sham acupuncture [nonelectrical acupuncture at Zusanli-Xiajuxu (stomach meridian, St 36–39), △], control acupuncture [nonelectrical and acupuncture at Guangming-Xuanzhong (gallbladder meridien, Gb 37–39), ○], and control electroacupuncture [electrical acupuncture at Gb 37–39, ●] trials in *protocol 2*. Data include periods of baseline (1 min), electroacupuncture (8 min), and recovery (1 min). Each data point represents average values over 1 min.

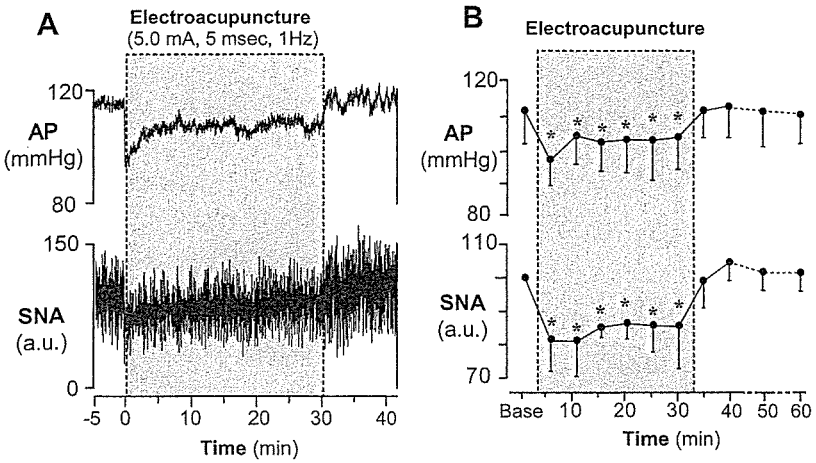

Fig. 6. Typical time series of AP and SNA during 30 min of 1-Hz electroacupuncture (St 36–39; *A*) and the averaged (n = 6) AP and SNA (*B*) in *protocol 3*. Data include periods of baseline (5 min), electroacupuncture (30 min), and recovery (30 min). Each data point represents averaged values over 5 min during baseline, electroacupuncture, and the first 10 min of recovery and those over 10 min during the last 20 min of recovery. *$P < 0.05$: significantly different from baseline after acupuncture insertion.

Another explanation for resetting in the neural arc may be circulatory endogenous opioids (e.g., β-endorphin and enkephalin), which are released from the adrenal gland and hypothalamus by prolonged (>30 min) electroacupuncture (20, 21). These endogenous opioids are known to modulate the arterial baroreflex (24, 29, 35). However, changes in endogenous opioids are unlikely to be the mechanism for reductions in SNA and AP by electroacupuncture in the present experimental settings because the inhibitory effects terminated immediately after cessation of electroacupuncture rather than lasting for several hours (42) (Fig. 1).

Previous studies suggest a central interaction between an electroacupuncture-evoked somatosympathetic reflex and the arterial baroreflex. Baroreceptor afferent inputs inhibit neural activities in the rostral ventrolateral medulla (rVLM) (6, 33). Tjen-A-Looi et al. (36) showed that electroacupuncture inhibited rVLM neural activities, suggesting that the electroacupuncture-evoked somatosympathetic reflex and arterial baroreflex share common central pathways. In addition, 2-Hz electroacupuncture inhibits SNA through the excitation of β-endorphinergic and GABAergic neurons to rVLM (12, 13).

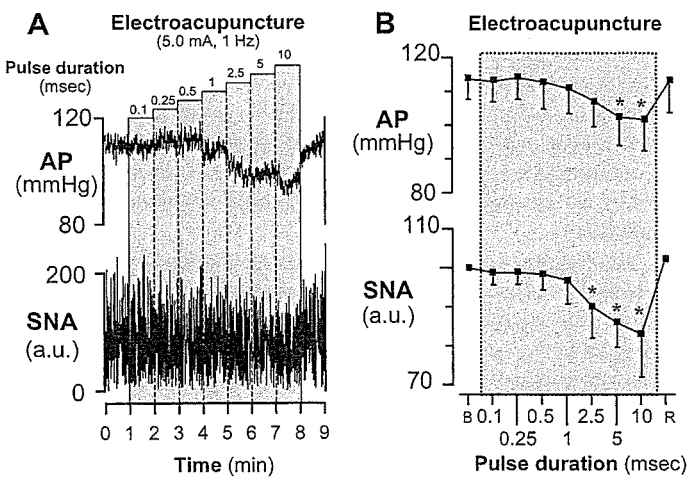

Fig. 7. Typical time series of AP and SNA during 1-Hz electroacupuncture with increasing the pulse duration (*A*) and the averaged (n = 6) AP and SNA (*B*) in *protocol 4*. Data include periods of baseline (B, 1 min), electroacupuncture (7 min), and recovery (R, 1 min). Each data point represents average values over 1 min. *$P < 0.05$; significantly different from baseline after acupuncture insertion.

Central interaction in the brain stem may be involved in the resetting of the arterial baroreflex neural arc induced by electroacupuncture.

Characteristics of Zusanli-Xiajuxu Electroacupuncture Used in the Present Study

The Zusanli electroacupuncture used in this study has some unique characteristics. First, our results showed that baseline AP and SNA were decreased significantly by electroacupuncture, in contrast to previous studies that found no significant reduction in baseline AP and SNA during Zusanli electroacupuncture in rats (0.5-ms duration, 1–2 mA, 2 Hz) (18) and nonelectrical acupuncture in normotensive humans (right large intestine 4, right liver 3, and left spleen 6) (22). Second, our result showed that AP and SNA were reduced as soon as electroacupuncture was started, in contrast to previous reports that the effect of Zusanli electroacupuncture did not even begin to manifest for the first 10–15 min in rats (0.5-ms duration, 1–2 mA, 2 Hz) (18) and cats (0.5-ms duration, 0.4–0.6 mA, 2–4 Hz) (37). These discrepancies may be related to the differences in acupoints and stimulation conditions (pulse duration, current, and frequency). In particular, the pulse duration used in our study (5 ms) was approximately 10–50 times longer than that used in previous studies. Indeed, the data obtained from *protocol 4* show that increasing the pulse duration augments the reduction in AP and SNA during electroacupuncture; pulse durations shorter than 2.5 ms did not change AP and SNA, whereas durations of 2.5 ms and above decreased both parameters immediately after the electroacupuncture was started (Fig. 7). In addition, our data suggest that stimulation duration (<2.5 ms) does not affect arterial baroreflex, consistent with our preliminary data that baroreflex neural, peripheral, and total arcs remained unchanged during electroacupuncture with pulse durations <2.5 ms (unpublished data). These observations may indicate that the effect of electroacupuncture on arterial baroreflex is linked to the stimulation pulse duration.

The third characteristic is that the inhibitory effects of electroacupuncture on AP and SNA disappeared immediately after the cessation of electroacupuncture. In contrast, some studies showed that the inhibitory effects of electroacupuncture on AP lasted for 10–60 min after the cessation (18). The characteristics in this study may not be explained by the length of electroacupuncture because AP and SNA recovered to the

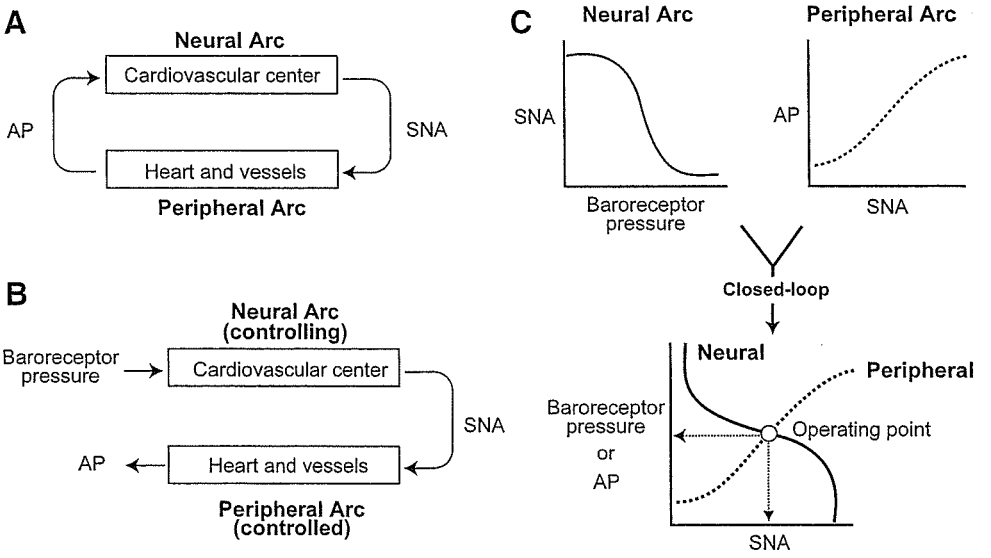

Fig. 8. Arterial baroreflex system in closed-loop (*A*) and open-loop (*B*) conditions. In open-loop conditions, the relationships between baroreceptor pressure and SNA (the neural arc) and between SNA and AP (the peripheral arc) can be quantitatively measured. Intersection of the neural and peripheral arcs corresponds to the operating point of AP and SNA under closed-loop conditions of feedback (*C*).

prestimulation baseline levels immediately after the cessation in both short-duration (8 min, Fig. 1) and longer-duration electroacupuncture (30 min, Fig. 6) protocols. The rapid disappearance of effects suggests that the AP and SNA reductions seen in the present study may not be elicited by the opioid mechanism, although clinical experiments with longer-duration electroacupuncture have demonstrated long-lasting effects on the cardiovascular system, which are attributed to opioid substances (2, 12, 15, 37, 42).

The reductions in AP and SNA during Zusanli electroacupuncture seen in the present study may not be just a nonspecific response to acupunctures. Our data from *protocol 2* (Fig. 5) showed that nonelectrical acupuncture at Zusanli (sham acupuncture) did not decrease AP and SNA, suggesting that the AP and SNA reductions during Zusanli electroacupuncture are not simply the results from insertion of acupuncture needles. Furthermore, acupuncture at Guangming-Xuanzhong (control acupuncture, control electroacupuncture) did not change AP and SNA regardless of electrical stimulation (Fig. 5). This result suggests the importance of acupoint specificity and is consistent with an earlier study showing point-specific differences in cardiovascular inhibitory responses (Jiangshi-Neiguan or Shousanli-Quchi acupoints vs. Pianli-Wenlui or Zusanli-Shangjuxu acupoints) (37). These observations may support the concept that Zusanli acupuncture changes cardiovascular variables in experimental animal models (4, 25, 28) and confers beneficial effects on cardiovascular diseases (5, 30, 34), whereas Guangming-Xuanzhong acupuncture does not affect cardiovascular variables (18).

Limitations

There are several limitations to this study. First, as anesthesia affects the autonomic nervous system, the results might have been different without anesthesia. Second, our isolation of the carotid sinus regions may stimulate carotid chemoreceptors. However, in determining baroreflex function, this factor was present in trials with and without electroacupuncture. Therefore, we believe that this factor may not affect our conclusion of baroreflex resetting during electroacupuncture.

Third, acupuncture was inserted at a point corresponding to the Zusanli acupoint in humans. When acupuncture is properly inserted at the acupoint, the patient feels heaviness or soreness. Such sensory information is not available in an anesthetized animal. Because electroacupuncture (as distinct from acupuncture with no electrical stimulation) stimulates not only the inserted point but also the surrounding area, it has been used as a convenient way of stimulating acupoints in patients and in experimental animals. Thus, even if we failed to insert the needle at the precise acupoint, we believe that Zusanli could be stimulated electrically.

Fourth, although we determined the effects of electroacupuncture at Zusanli acupoints on cardiovascular and baroreflex systems, there are other important acupoints that are able to influence these systems. In particular, Neiguan electroacupuncture is actually known to decrease sympathetic premotor neuron activity for a longer period than Zusanli electroacupuncture (36, 37). Further studies are necessary to determine the effect of Neiguan electroacupuncture on the arterial baroreflex.

Last, we evaluated the effects of Zusanli electroacupuncture on the baroreflex function for a short acupuncture duration of only 8 min. Because electroacupuncture is typically practiced for longer periods of time, our results have limited applicability. However, the electroacupuncture we used decreased AP and SNA immediately after application, showing that the procedure has acute effect on the cardiovascular system. That was the reason why we focused on the effect of short duration electroacupuncture on the baroreflex system. Future study is necessary to examine the effects of longer-duration electroacupuncture.

In conclusion, 1 Hz, short-term electroacupuncture of Zusanli reset the baroreflex neural arc toward lower SNA but did not affect the peripheral arc. The closed-loop operating point determined by the intersection of the neural and peripheral arcs was moved toward lower SNA and AP by electroacupuncture.

APPENDIX

Theoretical Considerations: Coupling of Neural and Peripheral Arcs

Changes in AP are immediately sensed by arterial baroreceptors, which alter efferent SNA via the cardiovascular center of baroreflex (Fig. 8*A*). Efferent SNA in turn governs heart rate and the mechanical

properties of the heart and vessels, which themselves exert a direct influence over AP. This negative-feedback loop makes it difficult to analyze the behavior of the arterial baroreflex. To overcome this problem, we opened the negative-feedback loop and divided the system into controlling and controlled elements (31). We defined the controlling element as the neural arc and the controlled element as the peripheral arc (Fig. 8*B*). In the neural arc, the input is the pressure sensed by the arterial baroreceptors and the output is SNA. In the peripheral arc, the input is SNA and the output is AP (Fig. 8*C*). Because pressure sensed by the arterial baroreceptor is equilibrated with AP under physiological conditions, we superimposed the functions of the two arcs and determined the operating point of the system from the intersection of the two arcs. The operating point is defined as the AP and SNA under closed-loop conditions of the feedback system. The validity of this framework has been examined in previous studies (10, 31). Using the baroreflex equilibrium diagram, we aimed to quantify the effects of electroacupuncture on the arterial baroreflex.

GRANTS

This study was supported by Health and Labor Sciences Research Grant for Research on Advanced Medical Technology from the Ministry of Health, Labour, and Welfare of Japan (H14-Nano-002), by a Grant-in-Aid for Scientific Research (A) (15200040) from the Japan Society for the Promotion of Science, the Program for Promotion of Fundamental Studies in Health Science from the Pharmaceutical and Medical Devices Agency of Japan, and by the "Ground-based Research Announcement for Space Utilization" project promoted by Japan Space Forum. This study was also supported by Industrial Technology Research Grant Program in 03A47075 from New Energy and Industrial Technology Development Organization (NEDO) of Japan.

REFERENCES

1. **Brickman AL, Calaresu FR, and Mogenson GJ.** Bradycardia during stimulation of the septum and somatic afferents in the rabbit. *Am J Physiol Regul Integr Comp Physiol* 236: R225–R230, 1979.
2. **Chao DM, Shen LL, Tjen-A-Looi S, Pitsillides KF, Li P, and Longhurst JC.** Naloxone reverses inhibitory effect of electroacupuncture on sympathetic cardiovascular reflex responses. *Am J Physiol Heart Circ Physiol* 276: H2127–H2134, 1999.
3. **Chen S and Ma SX.** Nitric oxide in the gracile nucleus mediates depressor response to acupuncture (ST36). *J Neurophysiol* 90: 780–785, 2003.
4. **Chiu DTJ and Cheng KK.** A study of the mechanism of the hypotensive effect of acupuncture in the rat. *Am J Chin Med* 2: 413–419, 1974.
5. **Chiu YJ, Chi A, and Reid IA.** Cardiovascular and endocrine effects of acupuncture in hypertensive patients. *Clin Exp Hypertens* 19: 1047–1063, 1997.
6. **Dampney RA, Horiuchi J, Tagawa T, Fontes MA, Potts PD, and Polson JW.** Medullary and supramedullary mechanisms regulating sympathetic vasomotor tone. *Acta Physiol Scand* 177: 209–218, 2003.
7. **Johansson B.** Studies on cardiovascular responses induced by electrical stimulation of afferent somatic nerves. A preliminary report. *Med Exp Int J Exp Med* 5: 447–453, 1961.
8. **Johansson B.** Circulatory responses to stimulation of somatic afferents with special reference to depressor effects from muscle nerves. *Acta Physiol Scand Suppl* 198: 1–91, 1962.
9. **Johansson B, Lundgren O, and Mellander S.** Reflex influence of "somatic pressor and depressor afferents" on resistance and capacitance vessels and on transcapillary fluid exchange. *Acta Physiol Scand* 62: 280–286, 1964.
10. **Kawada T, Shishido T, Inagaki M, Zheng C, Yanagiya Y, Uemura K, Sugimachi M, and Sunagawa K.** Estimation of baroreflex gain using a baroreflex equilibrium diagram. *Jpn J Physiol* 52: 21–29, 2002.
11. **Kent BB, Drane JW, Blumenstein B, and Manning JW.** A mathematical model to assess changes in the baroreceptor reflex. *Cardiology* 57: 295–310, 1972.
12. **Ku YH and Chang YZ.** β-Endorphin- and GABA-mediated depressor effect of specific electroacupuncture surpasses pressor response of emotional circuit. *Peptides* 22: 1465–1470, 2001.
13. **Ku YH and Zou CJ.** Beta-endorphinergic neurons in nucleus arcuatus and nucleus tractus solitarii mediated depressor-bradycardia effect of "Tinggong" 2-Hz electroacupuncture. *Acupunct Electrother Res* 18: 175–184, 1993.
14. **Legramante JM, Raimondi G, Adreani CM, Sacco S, Iellamo F, Peruzzi G, and Kaufman MP.** Group III muscle afferents evoke reflex depressor responses to repetitive muscle contractions in rabbits. *Am J Physiol Heart Circ Physiol* 278: H871–H877, 2000.
15. **Li L, Yin-Xiang C, Hong X, Peng L, and Da-Nian Z.** Nitric oxide in vPAG mediates the depressor response to acupuncture in stress-induced hypertensive rats. *Acupunct Electrother Res* 26: 165–170, 2001.
16. **Li P.** The effect of acupuncture on blood pressure: the interrelation of sympathetic activity and endogenous opeoid peptides. *Acupunct Electrother Res* 8: 45–56, 1983.
17. **Li P, Pitsillides KF, Rendig SV, Pan HL, and Longhurst JC.** Reversal of reflex-induced myocardial ischemia by median nerve stimulation: a feline model of electroacupuncture. *Circulation* 97: 1186–1194, 1998.
18. **Li P, Rowshan K, Crisostomo M, Tjen-A-Looi SC, and Longhurst JC.** Effect of electroacupuncture on pressor reflex during gastric distension. *Am J Physiol Regul Integr Comp Physiol* 283: R1335–R1345, 2002.
19. **Li P, Tjen-A-Looi S, and Longhurst JC.** Rostral ventrolateral medullary opioid receptor subtypes in the inhibitory effect of electroacupuncture on reflex autonomic response in cats. *Auton Neurosci* 89: 38–47, 2001.
20. **Lin JG, Chang SL, and Cheng JT.** Release of beta-endorphin from adrenal gland to lower plasma glucose by the electroacupuncture at Zhongwan acupoint in rats. *Neurosci Lett* 326: 17–20, 2002.
21. **Lin JG, Lo MW, Wen YR, Hsieh CL, Tsai SK, and Sun WZ.** The effect of high and low frequency electroacupuncture in pain after lower abdominal surgery. *Pain* 99: 509–514, 2002.
22. **Middlekauff HR, Yu JL, and Hui K.** Acupuncture effects on reflex responses to mental stress in humans. *Am J Physiol Regul Integr Comp Physiol* 280: R1462–R1468, 2001.
23. **Mohrman DE and Heller LJ.** *Cardiovascular Physiology* (4th ed.). New York: McGraw-Hill, 1997, p. 158–230.
24. **Moore PG, Quail AW, Cottee DB, McIlveen SA, and White SW.** Effect of fentanyl on baroreflex control of circumflex coronary conductance. *Clin Exp Pharmacol Physiol* 27: 1028–1033, 2000.
25. **Mori H, Uchida S, Ohsawa H, Noguchi E, Kimura T, and Nishijo K.** Electro-acupuncture stimulation to a hindpaw and a hind leg produces different reflex responses in sympathoadrenal medullary function in anesthetized rats. *J Auton Nerv Syst* 79: 93–98, 2000.
26. **Nishijo K, Mori H, Yosikawa K, and Yazawa K.** Decreased heart rate by acupuncture stimulation in humans via facilitation of cardiac vagal activity and suppression of cardiac sympathetic nerve. *Neurosci Lett* 227: 165–168, 1997.
27. **Ohsawa H, Okada K, Nishijo K, and Sato Y.** Neural mechanism of depressor responses of arterial pressure elicited by acupuncture-like stimulation to a hindlimb in anesthetized rats. *J Auton Nerv Syst* 51: 27–35, 1995.
28. **Ohsawa H, Yamaguchi S, Ishimaru H, Shimura M, and Sato Y.** Neural mechanism of pupillary dilation elicited by electro-acupuncture stimulation in anesthetized rats. *J Auton Nerv Syst* 64: 101–106, 1997.
29. **Petty MA and Reid JL.** The effect of opiates on arterial baroreceptor reflex function in the rabbit. *Naunyn Schmiedebergs Arch Pharmacol* 319: 206–211, 1982.
30. **Richter A, Herlitz J, and Hjalmarson A.** Effect of acupuncture in patients with angina pectoris. *Eur Heart J* 12: 175–178, 1991.
31. **Sato T, Kawada T, Inagaki M, Shishido T, Takaki H, Sugimachi M, and Sunagawa K.** New analytic framework for understanding sympathetic baroreflex control of arterial pressure. *Am J Physiol Heart Circ Physiol* 276: H2251–H2261, 1999.
32. **Si QM, Wu GC, and Cao XD.** Effects of electroacupuncture on acute cerebral infarction. *Acupunct Electrother Res* 23: 117–124, 1998.
33. **Sved AF, Ito S, and Madden CJ.** Baroreflex dependent and independent roles of the caudal ventrolateral medulla in cardiovascular regulation. *Brain Res Bull* 51: 129–133, 2000.
34. **Tam KC and Yiu HH.** The effect of acupuncture on essential hypertension. *Am J Chin Med* 3: 369–375, 1975.
35. **Taneyama C, Goto H, Kohno N, Benson KT, Sasao J, and Arakawa K.** Effects of fentanyl, diazepam, and the combination of both on arterial baroreflex and sympathetic nerve activity in intact and baro-denervated dogs. *Anesth Analg* 77: 44–48, 1993.
36. **Tjen-A-Looi SC, Li P, and Longhurst JC.** Prolonged inhibition of rostral ventral lateral medullary premotor sympathetic neurons by electroacupuncture in cats. *Auton Neurosci* 106: 119–131, 2003.

37. **Tjen-A-Looi SC, Peng L, and Longhurst JC.** Medullary substrate and differential cardiovascular responses during stimulation of specific acupoints. *Am J Physiol Regul Integr Comp Physiol* 287: R852–R862, 2004.
38. **Wang JD, Kuo TB, and Yang CC.** An alternative method to enhance vagal activities and suppress sympathetic activities in humans. *Auton Neurosci* 100: 90–95, 2002.
39. **Wong AM, Leong CP, Su TY, Yu SW, Tsai WC, and Chen CP.** Clinical trial of acupuncture for patients with spinal cord injuries. *Am J Phys Med Rehabil* 82: 21–27, 2003.
40. **Wong AM, Su TY, Tang FT, Cheng PT, and Liaw MY.** Clinical trial of electrical acupuncture on hemiplegic stroke patients. *Am J Phys Med Rehabil* 78: 117–122, 1999.
41. **Yamamoto K, Kawada T, Kamiya A, Takaki H, Miyamoto T, Sugimachi M, and Sunagawa K.** Muscle mechanoreflex induces the pressor response by resetting the arterial baroreflex neural arc. *Am J Physiol Heart Circ Physiol* 286: H1382–H1388, 2004.
42. **Yao T.** Acupuncture and somatic nerve stimulation: mechanism underlying effects on cardiovascular and renal activities. *Scand J Rehabil Med Suppl* 29: 7–18, 1993.

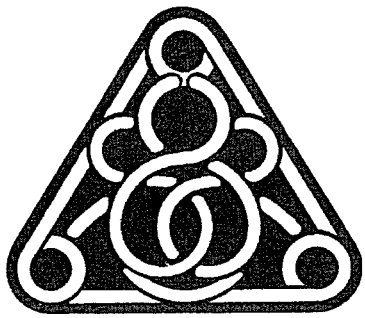

ARTICLE IN PRESS

ELSEVIER

International Journal of Cardiology xx (2005) xxx – xxx

International Journal of Cardiology

www.elsevier.com/locate/ijcard

Postexercise VO_2 "Hump" phenomenon as an indicator for inducible myocardial ischemia in patients with acute anterior myocardial infarction

Hiroshi Takaki [a,*], Satoru Sakuragi [b], Noritoshi Nagaya [b], Shoji Suzuki [b], Yoichi Goto [b], Takayuki Sato [c], Kenji Sunagawa [a]

[a] *Department of Cardiovascular Dynamics, National Cardiovascular Center Research Institute, 5-7-1 Fujishiro-dai, Suita, Osaka, 565-8565, Japan*
[b] *Division of Cardiology, Department of Internal Medicine, National Cardiovascular Center, Suita, Japan*
[c] *Department of Cardiovascular Control, Kochi Medical School, Nankoku, Japan*

Received 13 October 2004; received in revised form 30 May 2005; accepted 24 July 2005

Abstract

Objectives: At exercise testing with respiratory gas analysis in patients with inducible myocardial ischemia, we have occasionally observed abnormal transient oxygen uptake (VO_2) components with a characteristic "Hump"-shaped morphology early after exercise, which may serve as an index for inducible ischemia. We examined this hypothesis in patients with anterior q-wave myocardial infarction in whom the accuracy to identify ischemia by exercise ECG is limited.

Design: From patients with acute anterior q-wave infarction but without clinically overt heart failure who underwent pre-discharge exercise testing, we examined patients with (Group-I, $n=30$) and without (Group-N, $n=29$) inducible ischemia. To identify "Hump", postexercise VO_2 (up to 4 min) standardized for peak VO_2 was exponentially fitted with use of peak VO_2 and VO_2 of 90–240 s, yielding "expected VO_2". "D-curve" was obtained by subtracting "expected VO_2" from measured VO_2.

Results: Although exercise-induced ST depressions more frequently appeared in Group-I (27%) than in Group-N (3%, $p<0.05$), the prevalence was low. D-curve peaked later ($p<0.01$) and its value was greater ($p<0.05$) in Group-I than in Group-N. When "Hump" was defined to be present if D-curve peaked ≥ 40 s and its peak value $\geq 15\%$, it was far more frequently found in Group-I ($n=17/30$) than in Group-N ($n=1/29$, $p<0.01$). Thus, "Hump" could diagnose inducible ischemia with a sensitivity of 57% and a specificity of 97%.

Conclusions: Although not highly sensitive, postexercise VO_2 "Hump" with its peak occurring around 60 s after exercise is a specific marker for inducible ischemia. The identification may be useful, particularly in patients with limited accuracy of exercise ECG such as those with q-wave anterior infarction.

© 2005 Elsevier Ireland Ltd. All rights reserved.

Keywords: Exercise test; Respiratory gas analysis; Myocardial ischemia; Oxygen uptake

1. Introduction

In patients after acute myocardial infarction, the evaluation of inducible myocardial ischemia is important in the subsequent management, [1–3]] however, the diagnostic accuracy of exercise ECG is known to be limited in those patients [4–8]]. This is particularly crucial in patients with q-wave anterior infarction, in whom exercise-induced ST-segment depression would be often obscured by the presence of q-wave in the precordial leads.

Exercise testing with respiratory gas analysis is most often performed for evaluating the functional capacity and predicting prognosis in patients with heart failure, however, we have conducted the test in a considerable number of these post-infarct patients (approximately 200 tests/year) in our institute for more than 10 years [9]. Although the concomitant use of respiratory gas analysis is conducted mainly for the same purpose as above, postexercise oxygen uptake (VO_2) kinetics may provide useful information for detecting inducible ischemia in these patients. In practice,

* Corresponding author. Tel.: +81 6 6833 5012; fax: +81 6 6835 5403.
E-mail address: htakaki@res.ncvc.go.jp (H. Takaki).

0167-5273/$ - see front matter © 2005 Elsevier Ireland Ltd. All rights reserved.
doi:10.1016/j.ijcard.2005.07.012

ARTICLE IN PRESS

we have occasionally observed abnormal components with a characteristic "Hump"-shaped morphology in the early portion of the postexercise VO_2 decay in some of patients with evidence of inducible ischemia. The mechanism is unclear, however, it is conceivable that this phenomenon may be caused by enhanced stroke volume following resolution of ischemia during exercise, that is presumably responsible for delayed recovery of postexercise systolic blood pressure in patients with ischemia [10–15].

Abnormal VO_2 kinetics after exercise has been reported in patients with heart failure due to left ventricular dysfunction [16–18]. However, to our knowledge, no studies have examined the significance of the abnormal VO_2 kinetics after exercise occurring in association with inducible ischemia. We thus examined the diagnostic utility of this phenomenon ("Hump") as an indicator for inducible ischemia in patients after acute anterior q-wave infarction without clinically overt heart failure.

2. Methods

2.1. Study population

From the consecutive inpatients with acute anterior q-wave myocardial infarction but without overt heart failure who underwent both pre-discharge exercise testing with respiratory gas analysis (within 3 weeks after the onset of infarction) and coronary angiography (approximately 4 weeks after the onset), we recruited the study population as follows. As a control group, we selected 29 patients (Group-N) who had no significant (>50% luminal diameter narrowing) stenosis in the coronary arteries at angiography, although 83% ($n=24/29$) of these patients had received percutaneous coronary intervention (PCI) during the acute phase of their infarction. It was assumed that this group did not have inducible ischemia. In 30 patients with abnormal coronary arteries, exercise thallium-201 scintigraphy (single-photon emission computed tomography; SPECT) showed reversible perfusion defects corresponding to the anatomic lesions demonstrated (Group-I). Of these patients, 43% ($n=13/30$) had received PCI during the acute phase, and at subsequent angiography 22 were left with single, five with double, and three with triple vessel disease (Table 1). All patients with Group-I subsequently received revascularization with either percutaneous transluminal angioplasty ($n=26$) or coronary artery bypass graft surgery ($n=4$).

We excluded patients with primary lung disease, orthopedic difficulties that precluded maximal exercise, arteriosclerotic obliterance and significant arrhythymias including atrial fibrillation. The patients with VO_2 plateau or leveling off (defined as an increase in VO_2 of less than 50 ml/min) around at peak exercise were also excluded ($n=2$), because the present study aimed to evaluate the significance of abnormal VO_2 kinetics ("Hump") only seen in the recovery period.

Table 1
Patients' characteristics

	Group-I ($N=30$)	Group-N ($N=29$)	p value
Sex (M/F)	26/4	22/7	NS
Age (years)	64±8	61±10	NS
LV EF (%)	39±7	43±9	NS
History of prior MI	7(23%)	2(7%)	NS
PCI therapy	13(43%)	24(83%)	<0.01
Coronary artery disease			
SVD	22(73%)	–	
DVD	5(17%)	–	
TVD	3(10%)	–	
Medication			
beta-blocker	13(43%)	6(21%)	NS
Ca antagonist	15(50%)	18(62%)	NS
Nitrate	21(70%)	10(34%)	<0.05
Digitalis	0 (0%)	2(7%)	NS

Values are expressed as mean±SD.
LVEF, left ventricular ejection fraction; MI, myocardial infarction; PCI, percutaneous coronary intervention; SVD, single vessel disease; DVD, double vessel disease; TVD, triple vessel disease.

Left ventricular ejection fraction (LVEF) was similar between the two groups (Table 1). There were no significant differences in sex, age, and history of prior myocardial infarction. The use of cardiovascular drugs was similar in the two groups except for nitrate, and it was neither altered nor withheld for the exercise test. All patients gave informed consent for the study.

2.2. Exercise testing

Symptom-limited exercise testing with respiratory gas analysis was performed on an upright bicycle ergometer in a ramp fashion. After a 2-min rest, exercise was begun with a 1-min warm up at 0 W at 60 rpm, followed by 15 W incremental loading every 1 min. ECGs (V_1, V_5, aV_F) and heart rate (HR) were monitored throughout the testing, while recording hardcopies of 12-lead ECG every 1 or 2 min. HR and blood pressure (BP) measured by a conventional cuff sphygmomanometer were recorded at rest, at 1-min intervals during exercise, and 1, 2, and 4 min into the recovery period. All patients stopped exercise because of dyspnea and/or leg fatigue, and there was no patient in whom exercise was stopped because of angina, marked ST-segment depressions or fall of blood pressure. Patients were asked to stop pedaling soon after exercise (up to 10 s) to avoid the possible influence of cool-down exercise on recovery VO_2 kinetics.

Expired gas was measured on a breath-by-breath basis at rest, during the exercise, and recovery period (at least up to 4 min) with a respiromonitor AE280 (Minato Medical Electronics, Osaka, Japan). The system was carefully calibrated before each study. VO_2, carbon dioxide production (VCO_2), and minute ventilation (VE) were stored in a computer hard disk every 6 s for later analysis.

We identified a significant ST-segment depression induced by exercise according to the following criteria; (1) a horizontal or downsloping ST-segment displacement at J-point $\geq$0.1 mV (2) up-sloping ST-segment displacement at 80 ms after the J-point $\geq$0.15 mV in at least 3 consecutive beats at peak exercise. A significant ST-segment elevation was defined as an upward shift of the ST-segment $\geq$0.1 mV at the J-point compared with the resting level.

2.3. Exercise SPECT

The test was performed with symptom-limited bicycle exercise. At near-maximal exercise, thallium-201 was intravenously injected and the patient was encouraged to exercise for another 1 min. SPECT images were obtained at 15 min (initial images) and 4 h (delayed images). The images were assessed by two experienced physicians unaware of the patient clinical information. Thallium uptake was classified as normal, mildly, moderately or severely reduced, or absent. A reversible defect was defined when the classification improved by at least one category from the initial to delayed image.

2.4. Data analysis

By using our custom-made software, we evaluated abnormal manifestations ("Hump") in early postexercise VO_2 decay (Fig. 1). To characterize "Hump", we performed the following procedures, assuming that postexercise VO_2 decay would normally (i.e., without inducible ischemia) follow an approximately exponential curve and that "Hump" would be expressed by the components that was not fitted by this approximation. We first standardized the time-series of VO_2 data following exercise up to 4 min for peak VO_2. The curve was monoexponentially fitted with use of peak VO_2 and continuous VO_2 data over the period of 90–240 s; i.e., the data from 6 to 90 s were excluded from the fitting because we had observed abnormal components in this period. Nonlinear least-squares fitting was made assuming a monoexponential model: $y=Z_0\times e^{-t/\mu}+Z_\infty$ (where y is the standardized VO_2 data, Z_0 is the initial standardized VO_2 above Z_∞, μ is the time constant, t is time after the termination of exercise and Z_∞ is the asymptote to which standardized VO_2 decay).

The fitted curve was termed the "expected VO_2 curve" in this study (Fig. 1). To characterize "Hump" phenomenon, we obtained the "D-curve" by subtracting the expected VO_2 curve from actually measured VO_2 curve. In the D-curve that was a function of time (every 6 s) after exercise, we determined the peak value (D_{max}) in amplitude and the elapsed time at the time point of D_{max} (T_{max}). These two indices were compared between the two groups.

Systolic BP and HR at rest, at peak exercise and at the recovery period of 1, 2, and 4 min after exercise were also analyzed.

2.5. Statistical analysis

Values are expressed as mean±SD. Between-group differences for unpaired values were analyzed by Student's t test and by the Mann–Whitney U test when appropriate. Repeated measures of analysis of variance were used to

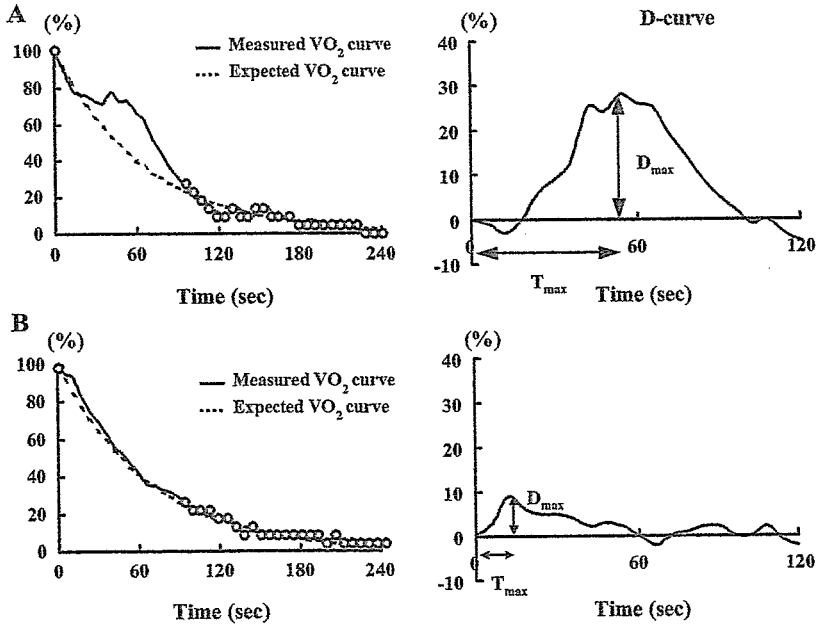

Fig. 1. Representative examples of postexercise VO_2 decay (left panel) and the derived D-curve (right panel) of two patients. Illustrated in the upper panels (A) are graphs for a patient of Group-I, and the lower (B) depict those for a patient of Group-N. After VO_2 decay curve standardized for peak VO_2 was exponentially fitted with use of peak VO_2 and VO_2 over the period of 90–240 s ("expected VO_2 curve", broken line), we obtained D-curve by subtracting "expected VO_2 curve" from actually measured VO_2 curve. In the D-curve, D_{max} (peak value) and T_{max} (time to peak) were estimated. VO_2=oxygen uptake.

ARTICLE IN PRESS

Table 2
Exercise variables

	Group-I (N=30)	Group-N (N=29)	p-value
Rest HR (bpm)	70±12	75±17	NS
Rest SBP (mm Hg)	128±26	119±16	NS
Duration of exercise (s)	510±66	553±87	<0.05
Exercise-induced angina	3(10%)	0(0%)	NS
Peak HR (bpm)	137±27	147±24	NS
Peak SBP (mm Hg)	174±25	178±25	NS
ECG change			
ST elevation	14(47%)	16(55%)	NS
ST depression	8(27%)	1(3%)	<0.05
Peak WR (watt)	113±19	123±22	NS
Peak VO_2 (ml/min)	1179±192	1335±278	<0.05

Values are expressed as mean±SD. HR, heart rate; SBP, systolic blood pressure; VO_2, oxygen uptake; WR, work rate.

compare the values during recovery period. When this test was significant, the Newman–Keuls post hoc test was performed for multiple comparisons. Difference in categorical variables was analyzed by chi-square analysis. A p-value <0.05 was considered statistically significant. Receiver operating characteristics curves (ROC) were used to assess the ability of T_{max} and D_{max} to diagnose inducible ischemia [19].

3. Results

3.1. Exercise testing results

Table 2 shows exercise parameters for Group-I and Group-N. There were no significant differences in rest HR, rest systolic BP (SBP), peak HR or peak SBP between the two groups. Although peak work rate was similar between the two groups, the duration of exercise was shorter and peak VO_2 was lower in Group-I than Group-N ($p<0.05$, both). However, these 2 parameters were of little help for differentiating the two groups; for instance, there was considerable overlap in peak VO_2 between the groups. Only 3 patients of Group-I complained of anginal symptoms after exercise.

As for ECG parameters, the frequency of a significant exercise-induced ST-segment elevation was comparable between Group-I and Group-N (47% and 55%, respectively). Despite the presence of inducible ischemia, a significant ST-segment depression was found in only 8 of 30 patients (27%) in Group-I, although it was more frequently observed in Group-I than in Group-N (27% vs. 3%, $p<0.05$).

3.2. Comparison of postexercise VO_2

To evaluate the overall difference in postexercise VO_2 decay (D-curve) between the 2 groups, we averaged the value of D-curve over every 30 s in the first 2 min of the recovery period (Fig. 2, upper two panels). As a result, the magnitude was significantly greater in the period of 30–60 s than in the period of 0–30 s in Group-I (13.7%±8.2% vs. 8.7%±5.1%, $p<0.01$, Fig. 2A), whereas such a difference was not observed in Group-N (11.0%±5.2% vs. 10.2%±5.0%, NS, Fig. 2B).

To characterize the "Hump" phenomenon in D-curve, the peak value (D_{max}) and its elapsed time (T_{max}) were compared between the groups. T_{max} was significantly longer in Group-I than in Group-N (42.6±14.6 vs. 31.2±13.2 s,

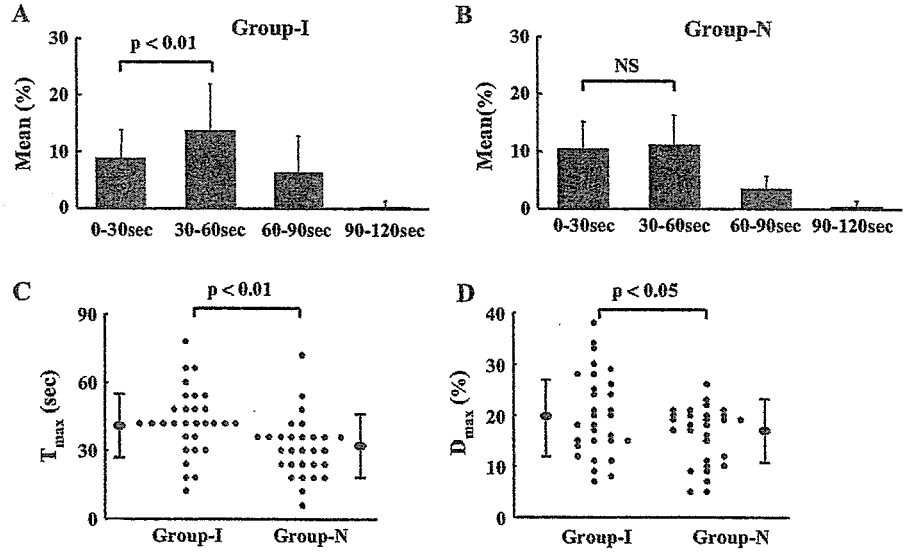

Fig. 2. The time-course changes in the D-curve for the first 2 min of recovery (upper panel) and comparisons of T_{max} (C, lower left panel) and D_{max} (D, lower right panel) between Group-I and Group-N. The D-curve values averaged over every 30 s were shown as bar graphs for Group-I (A, upper left panel) and Group-N (B, upper right panel). The mean for 30–60 s was greater than that for 0–30 s in Group-I ($p<0.01$), but not in Group-N. T_{max} was longer in Group-I than in Group-N ($p<0.01$), and D_{max} was greater in Group-I than in Group-N ($p<0.05$).

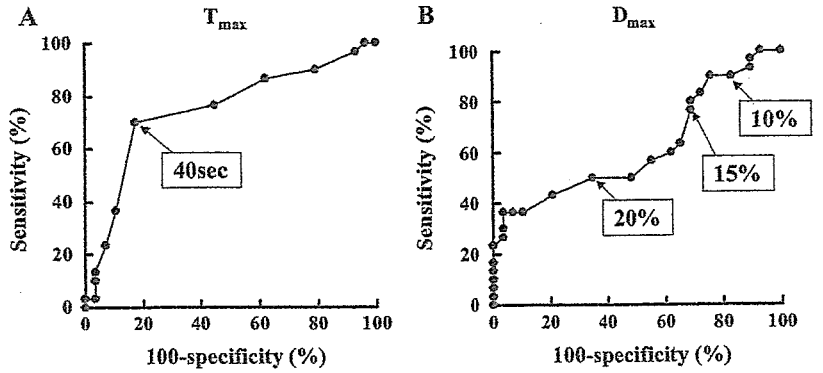

Fig. 3. ROC curves describing the ability for the diagnosis for inducible ischemia using T_{max} (A, left panel) and D_{max} (B, right panel).

$p<0.01$, Fig. 2C), and D_{max} was also significantly greater in Group-I than in Group-N (20.1%±8.1% vs. 16.2%±5.7%, $p<0.05$, Fig. 2D).

We used ROC analysis to determine the optimum cutoff values of these two parameters for identifying Hump phenomenon, i.e., inducible ischemia. When ROC analysis was conducted separately for T_{max} (Fig. 3A) and D_{max} (Fig. 3B), we could easily recognize 40 s as the optimum cutoff for T_{max} in differentiating the two groups, whereas such an optimum point was not found for D_{max}. Since it is considered that the combination of the two optimum cutoff values, each of which was determined by a separate ROC analysis, would not necessarily have the highest discriminative power, ROC analysis of T_{max} was repeated for a given D_{max}, while shifting D_{max} every 1% from 0% to 40%. As a result, when assuming that the best cutoff was defined as the point with highest sum of sensitivity and specificity, the combination of $D_{max} \geq 10\%$ and $T_{max} \geq 40$ s (from 37 to 41 s, because temporal resolution was 6 s) could most accurately discriminate Group-I from Group-N (sensitivity 67%, specificity 90%, accuracy 78%, Table 3). When $D_{max} \geq 15\%$ was applied (Fig. 4), the specificity was increased to 97%, although the sensitivity decreased to 57%.

3.3. Comparison of postexercise SBP

Although resting and peak SBP were not different between the two groups, Group-I had a higher SBP than Group-N at 2 and 4 min of recovery (both $p<0.05$, Fig. 5A).

Furthermore, among patients of Group-I, patients with "Hump", defined as $T_{max} \geq 40$ s and $D_{max} \geq 15\%$, had a higher SBP at 1 and 2 min of recovery than those without "Hump" (both $p<0.05$, Fig. 5B). A significant decrease in SBP from peak exercise was found at 1 min of recovery in patients without "Hump", but not in those with "Hump".

Table 3
Diagnostic accuracy of "Hump" for identifying inducible ischemia (Group-I)

T_{max} (s)	≥40	≥40	≥40
D_{max} (%)	≥10	≥15	≥20
Sensitivity	67% (20/30)	57% (17/30)	37% (11/30)
Specificity	90% (26/29)	97% (28/29)	100% (29/29)
Accuracy	78%	76%	68%

4. Discussion

Although exercise-induced ST-segment depression is a cardinal index to identify inducible myocardial ischemia on exercise testing, the diagnostic accuracy by the standard ST criteria is limited in post-infarct patients [4–8]. In our population consisting of patients after acute anterior q-wave myocardial infarction, ST-segment depressions during exercise appeared in only 27% of patients with inducible myocardial ischemia (Group-I), that was comparable to the incidence of ST depression reported previously [6–8]. The most likely explanation for the low sensitivity of ST depression in these patients is that exercise-induced ST elevation over q-wave leads, related to left ventricular asynergy, would mask the appearance of ST depression [5,20]. In patients with anterior q-wave myocardial infarction, the vector of ST-segment depression, which most frequently appears in the left precordial leads of V_4 to V_6,

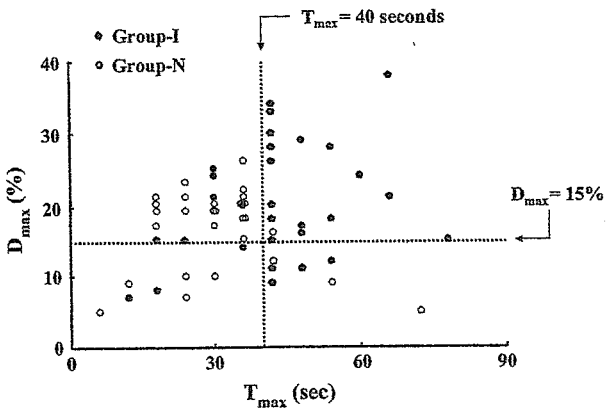

Fig. 4. Scatterplots showing D_{max} plotted against T_{max} for each patient. Approximately half (57%) of patients of Group-I (closed circle) were distributed in the limited area of $T_{max} \geq 40$ s and $D_{max} \geq 15\%$, whereas only one patient in Group-I (open circle) was distributed in this area. Using this criterion, we could diagnose the presence of inducible ischemia (Group-I) with a sensitivity of 57% and a specificity of 97%.

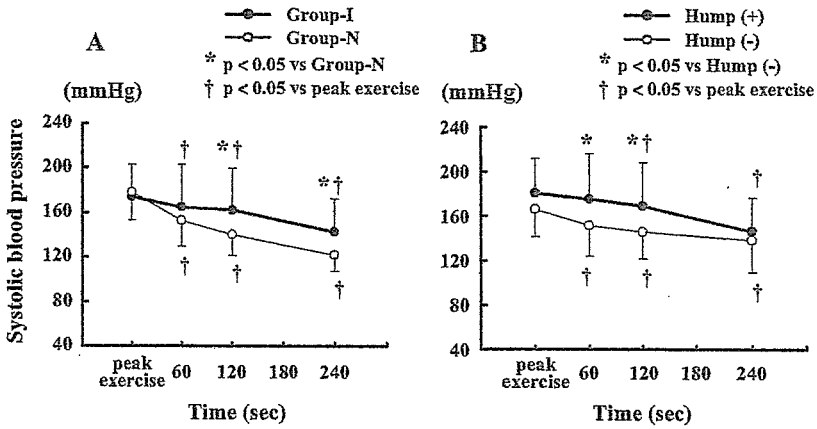

Fig. 5. Comparisons of systolic blood pressure time-course after exercise between Group-I and Group-N (A, left panel), and between the Group-I patients with and without "Hump" phenomenon (B, right panel).

may be electrically canceled by the opposite vector of ST elevation occurring in association with ventricular asynergy.

It is generally accepted that exercise-induced ST-segment elevation over post-infarct q-wave leads occurs in association with severe left ventricular asynergy, however, several studies indicated that exercise-induced ST-segment elevation might occur due to induced ischemia [21,22]. In the present study, we observed a similar prevalence of ST-segment elevation of ≥ 0.1 mV in Group-N (55%) and Group-I (47%, NS), suggesting that this index alone is of no use for identifying ischemia. We cannot exclude the possibility that ST-segment elevation might be caused by ischemia in some patients of Group-I, because three Group-I patients presented both exercise-induced ST-segment elevation and depression.

On the other hand, the present study has shown that abnormal transient VO_2 components after exercise, "Hump" phenomenon defined by our method described above, is a useful indicator for inducible ischemia in patients with acute anterior infarction. When the combination of $T_{max} \geq 40$ s and $D_{max} \geq 15\%$ were used for the definition of "Hump", we could diagnose inducible ischemia with sensitivity of 57%, specificity of 97%.

Abnormal postexercise VO_2 kinetics has been reported previously in patients with cardiocirculatory disorders. Hayasida et al. and other authors reported that the recovery of VO_2 was prolonged in patients with left ventricular dysfunction and that the time-course of VO_2 decay after exercise was closely related to exercise capacity [16–18,23–27] and prognosis [28]. Delayed energy store recovery in the skeletal muscle [22,24] and prolonged decrease in cardiac output [23,25–27,29] are considered to be involved in the genesis of this abnormal VO_2 recovery.

To our knowledge, there have been no published studies specifically examining the significance of exercise-induced ischemia on the postexercise abnormal VO_2 kinetics. Abnormal components of our interest, i.e., "Hump", is characterized by a transient convex bulge in the limited portion of VO_2 decay at around 1 min. The occurrence seems to appear not immediately but soon after the termination of exercise, generally lasting approximately 1 min. Previous reports estimated abnormal VO_2 kinetics by estimating the whole VO_2 decay with use of temporal parameters such as half time, [18,24,26] time constant [16,23,25] or cumulative area [28]. Since these measures are clearly unsuitable for our purpose, the non-exponential components (i.e., D-curve), that were derived by subtraction assuming that the abnormal components would be superimposed upon the monoexponential VO_2 decay, were compared between Group-I and Group-N. As a result, in Group-I, the mean value averaged over 30–60 s was greater than that averaged over 0–30 s, whereas such a difference was not found in Group-N (Fig. 2, upper two panels). Furthermore, the D-curve peaked later and its maximal value was greater in Group-I compared with Group-N (Fig. 2, lower two panels). Thus, the group difference of the D-curve with respect to the amplitude and temporal profile enabled us to identify the presence of inducible ischemia by the criterion shown in Table 3.

It was somewhat unexpected that some of patients without inducible ischemia (Group-N) showed a sizable amount of non-exponential components in the very early period of recovery up to 30 to 40 s. Our expectation was that non-exponential components in Group-N would be negligibly small, because the VO_2 decay curve should be closely fitted by the monoexponential model. This discrepancy indicates that postexercise VO_2 decay is not necessarily monoexponential in shape, and may be more precisely fitted by other mathematical models such as a sigmoidal model, even in the absence of inducible ischemia, although simple noise inherent in the measurements might be also related to the components. Impairment of LV function due to infarction and peripheral dysfunction caused by the immobilization (deconditioning effects) in the acute phase of myocardial infarction would contribute to the loss of the rapid fall of VO_2 immediately after exercise.

Several studies indicated that, in patients with inducible myocardial ischemia, an abnormal systolic blood pressure

response is observed not only during exercise but also during the recovery phase; a lesser decrease in systolic BP in the early recovery period, [10–15] which was in agreement with our results that the prolonged time-course of the postexercise decrease in systolic BP was seen in Group-I. It was also reported that, in these patients, stroke volume during exercise progressively decreased according to the development of severe ischemia, and it did not decrease but rather increased during the early period of recovery. [29–31] Although this paradoxical increase following exercise may occur either by a decrease in peripheral vascular tone after exercise [29,30] or by an improvement of LV function following the resolution of induced ischemia, [31] dynamic changes in the former factor are unlikely to transiently occur. The fact that, in Group-I, systolic BP at 1 min of recovery did not significantly decrease from peak exercise only in patients with "Hump", but not in patients without "Hump " reasonably suggests the direct role of enhanced stroke volume soon after exercise on the occurrence of "Hump".

The exact mechanism responsible for "Hump" is speculative, however, a recent study by Belardinelli et al. may provide a clue to the mechanism [32]. They indicated that exercise-induced ischemia resulting in a reduction in stroke volume decreases the increase rate of VO_2 to work rate increase (i.e., $\Delta VO_2/\Delta WR$) after the ischemic threshold. This reduction in $\Delta VO_2/\Delta WR$ would produce some amount of abnormal oxygen deficit (that is, extra-oxygen deficit), which might be paid back soon after exercise when the cardiac performance recovers. We consider that this process may be "Hump", transiently appearing on the limited portion of the early recovery of VO_2 decay. It should be noted that a reduction in $\Delta VO_2/\Delta WR$ during exercise was difficult to discern by visual inspection in any patient in our patients including those manifesting "Hump", probably because of a large spontaneous variations in VO_2 during exercise.

As described previously, it is possible that a mono-exponential curve used for deriving the non-exponential components is not be the most appropriate model for identifying "Hump". No single model may be suitable for fitting of the postexercise VO_2 decay, because the morphology of postexercise VO_2 decay curve considerably varied between individuals, probably due to the varying extent of impairment of LV function and the status of conditioning. Nevertheless, our method could identify "Hump" with a reasonable sensitivity and high specificity. Further investigation is necessary to ascertain this issue.

In conclusion, postexercise VO_2 "Hump" phenomenon, with its peak occurring around 60 s after exercise, seems to be a useful marker for inducible myocardial ischemia. The identification of this phenomenon may be more useful, particularly in patients with limited diagnostic accuracy of exercise ECG such as those with anterior myocardial infarction.

Acknowledgments

This study was supported by Research Grants for Cardiovascular Diseases (11C-7) from the Ministry of Health and Welfare of Japan, by Grant-in-Aid for Scientific Research (C-11670730) from the Japan Society for the Promotion of Science, and by the Program for Promotion of Fundamental Studies in Health Science from the Organization for Pharmaceutical Safety and Research.

References

[1] Taylor GJ, Humphries JO, Mellitis ED, et al. Predictors of clinical course, coronary anatomy and left ventricular function after recovery from acute myocardial infarction. Circulation 1980;62:960–70.
[2] Sanz G, Castoner A, Betriu A, et al. Determinants of prognosis in survivors of myocardial infarction: a prospective clinical angiographic study. N Engl J Med 1982;306:1065–70.
[3] De Feyter PJ, van Eeruge MJ, Dighton DH, et al. Prognostic value of exercise testing, coronary angiography and left ventriculography 6–8 weeks after myocardial infarction. Circulation 1982;66:527–36.
[4] Theruox P, Waters DD, Halpen C, et al. Prognostic value of exercise testing soon after myocardial infarction. N Engl J Med 1979;301: 341–5.
[5] Castellanet MJ, Greenberg PS, Ellestad MH. Comparison of ST-segment change on exercise testing with angiographic findings in patients with prior myocardial infarction. Am J Cardiol 1978;42: 29–35.
[6] Tilkemeier PL, Guiney TE, LaRaia PJ, et al. Prognostic value of predischarge low-level exercise thallium testing after thrombolytic treatment of acute myocardial infarction. Am J Cardiol 1990;66: 1203–7.
[7] Froelicher VF, Perdue ST, Atwood JE, et al. Exercise testing of patients recovering from myocardial infarction. Eur Probl Cardiol 1986;11:370–444.
[8] Haber HL, Beller GA, Watson DD, et al. Exercise thallium-201 scintigraphy after thrombolytic therapy with or without angiography for acute myocardial infarction. Am J Cardiol 1993;71:1257–61.
[9] Tomita T, Takaki H, Hara Y, et al. Attenuation of hypercapnic carbon dioxide chemosensitivity after postinfarction exercise training: possible contribution to the improvement in exercise hyperventilation. Heart 2003;9:404–10.
[10] Kato K, Saito F, Hatano K, et al. Prognostic value of abnormal postexercise systolic blood pressure response; prehospital discharge test after myocardial infarction in Japan. Am Heart J 1990;119: 264–71.
[11] Miyahara T, Yokota M, Iwase M, et al. Mechanism of abnormal postexercise systolic blood pressure response and its diagnostic value in patients with coronary artery disease. Am Heart J 1990;120:40–9.
[12] Tsuda M, Hatano K, Hayashi H, et al. Diagnostic value of postexercise systolic blood pressure response for detecting coronary artery disease in patients with or without hypertension. Am Heart J 1993;125:718–24.
[13] Abe K, Tsuda M, Hayashi H, et al. Diagnostic usefulness of postexercise systolic blood pressure response for detection of coronary artery disease in patients with electrocardiographic left ventricular hypertrophy. Am J Cardiol 1995;76:892–5.
[14] Hashimoto M, Okamoto M, Yamagata T, et al. Abnormal systolic blood pressure response during exercise recovery in patients with angina pectoris. J Am Coll Cardiol 1993;22:659–64.
[15] McHam SA, Marwick TH, Pashkow FJ, et al. Delayed systolic blood pressure recovery after graded exercise. J Am Coll Cardiol 1999; 34:754–9.

ARTICLE IN PRESS

[16] Hayashida W, Kumada T, Kohno F, et al. Post-exercise oxygen uptake kinetics in patients with left ventricular dysfunction. Int J Cardiol 1993;38:63–72.
[17] Riley M, Stanford CF, Nicholls DP. Ventilatory and heart rate responses after exercise in chronic cardiac failure. Clin Sci (Lond) 1994;87:231–8.
[18] Cohen-Solal A, Laperche T, Morvan D, et al. Prolonged kinetics of recovery of oxygen consumption after maximal graded exercise in patients with chronic heart failure. Circulation 1995;91:2924–32.
[19] Hanley JA, McNeil BJ. A method of comparing the areas under receiver operating characteristic curves derived from the same cases. Radiology 1983;148:839–43.
[20] Manvi KM, Ellestd MH. Elevated ST segments with exercise in ventricular aneurysm. J Electrocardiol 1972;5:317–23.
[21] Miyakado H, Kato M, Noguchi N, et al. Exercise-induced ST-segment elevation-role of left ventricular wall motion abnormalities and coronary artery narrowing. Jpn Circ J 1995;59:725–35.
[22] Feyter PJ, Majid PA, Eenige MJ, Wardeh R, Wempe FN, Roos JP. Clinical significance of exercise-induced ST segment elevation. Correlative angiographic study in patients with ischemic heart disease. Br Heart J 1981;6:84–92.
[23] Kitaoka H, Takata J, Furumo T, et al. Delayed recovery of postexercise blood pressure in patients with chronic heart failure. Am J Cardiol 1997;79:1701–4.
[24] Cohen-Solal A, Czitrom D, Geneves M, et al. Delayed attainment of peak oxygen consumption after the end of exercise in patients with chronic heart failure. Int J Cardiol 1997;60:23–9.
[25] Pavia L, Myers J, Cesare R. Recovery kinetics of oxygen uptake and heart rate in patients with coronary artery disease and heart failure. Chest 1999;116:808–13.
[26] Tanabe Y, Takahashi M, Hosaka Y, et al. Prolonged recovery of cardiac output after maximal exercise in patients with chronic heart failure. J Am Coll Cardiol 2000;35:1228–36.
[27] Daida H, Allison TG, Johnson BD, et al. Further increase in oxygen uptake during early active recovery following maximal exercise in chronic heart failure. Chest 1996;109:47–51.
[28] Groote P, Millaire A, Decoulx E, et al. Kinetics of oxygen consumption during and after exercise in patients with dilated cardiomyopathy. New markers of exercise intolerance with clinical implications. J Am Coll Cardiol 1996;28:168–75.
[29] Koike A, Ito H, Doi M, et al. Beat-to-beat evaluation of cardiac function during recovery from upright bicycle exercise in patients with coronary artery disease. Am Heart J 1990;120:316–23.
[30] Plotnick GD, Becker LC, Fisher ML, et al. Changes in left ventricular function during recovery from upright bicycle exercise in normal persons and in patients with coronary artery disease. Am J Cardiol 1986;58:247–51.
[31] Schneider RM, Weintraub WS, Klein LW, et al. Rate of left ventricular functional recovery by radionuclide angiography after exercise in coronary artery disease. Am J Cardiol 1986;57:927–32.
[32] Belardinelli R, Lacalaprice F, Carle F, et al. Exercise-induced myocardial ischaemia detected by cardiopulmonary exercise testing. Eur Heart J 2003;24:1304–13.

J Pharmacol Sci **101**, 214 – 222 (2006)

Journal of Pharmacological Sciences
©2006 The Japanese Pharmacological Society

Full Paper

Acetylcholine Inhibits the Hypoxia-Induced Reduction of Connexin43 Protein in Rat Cardiomyocytes

Yanan Zhang[1], Yoshihiko Kakinuma[2,*], Motonori Ando[2], Rajesh G Katare[2], Fumiyasu Yamasaki[1], Tetsuro Sugiura[1], and Takayuki Sato[2]

Departments of [1]Clinical Laboratory and [2]Cardiovascular Control, Kochi Medical School, Nankoku, Kochi 783-8505, Japan

Received December 14, 2005; Accepted May 8, 2006

Abstract. In a recent study, we demonstrated that vagal stimulation increases the survival of rats with myocardial infarction by inhibiting lethal arrhythmia through regulation of connexin43 (Cx43). However, the precise mechanisms for this effect remain to be elucidated. To investigate these mechanisms and the signal transduction for gap junction regulation, we investigated the effect of acetylcholine (ACh), a parasympathetic nerve system neurotransmitter, on the gap junction component Cx43 using H9c2 cells. When cells were subjected to hypoxia, the total Cx43 protein level was decreased. In contrast, pretreatment with ACh inhibited this effect. To investigate the signal transduction, cells were pretreated with L-NAME, a nitric oxide synthase inhibitor, followed by ACh and hypoxia. L-NAME was found to suppress the ACh effect. However, a NO donor, SNAP, partially inhibited the hypoxia-induced reduction in Cx43. To delineate the mechanisms of the decrease in Cx43 under hypoxia, cells were pretreated with MG132, a proteasome inhibitor. Proteasome inhibition produced a striking recovery of the decrease in the total Cx43 protein level under hypoxia. However, cotreatment with MG132 and ACh did not produce any further increase in the total Cx43 protein level. Functional studies using ACh or okadaic acid, a phosphatase inhibitor, revealed that both reagents inhibited the decrease in the dye transfer induced by hypoxia. These results suggest that ACh is responsible for restoring the decrease in the Cx43 protein level, resulting in functional activation of gap junctions.

Keywords: acetylcholine, connexin43, cardiomyocyte, hypoxia, proteasome inhibitor

Introduction

The prognosis of patients with chronic heart failure remains poor, despite the introduction of new pharmacological approaches and defibrillation devices, mainly due to lethal arrhythmia (1). Therefore, another therapeutic approach would be indispensable. In heart failure, the sympathetic nerve system is relatively activated compared with the parasympathetic nerve system (2), and this sympathetic nerve system-predominant condition is known to be involved in arrhythmogenicity. Recently, vagal nerve stimulation was reported to remarkably improve the survival rate of rats with heart failure due to myocardial infarction (3), suggesting that reactivation of the parasympathetic nerve system, which is suppressed in heart failure, plays a crucial role in attenuating the progression of heart failure. Moreover, our recent study revealed that acetylcholine (ACh), a parasympathetic nerve system neurotransmitter, plays an important role in regulating the protein level of the gap junction component connexin43 (Cx43) in the infarcted heart and cardiomyocytes under hypoxia (4). However, the precise mechanisms by which ACh regulates Cx43 remain to be elucidated. To investigate these mechanisms, we focused on Cx43 in H9c2 cells.

Gap junctions are intercellular junctions, and several connexin family members, including Cx43, participate in their formation. Among the connexin family members, Cx43 is the principal electrical coupling

*Corresponding author. kakinuma@med.kochi-u.ac.jp
Published online in J-STAGE: July 7, 2006
doi: 10.1254/jphs.FP0051023

protein in ventricles, while Cx40 plays the same role in atria. The functions of Cx43 are regulated by phosphorylation as well as the protein level. Cx43 phosphorylation can modulate the channel properties and turnover dynamics. SDS-PAGE of Cx43 generally reveals a faster non-phosphorylated isoform (NP-Cx43) and slower phosphorylated isoforms (P-Cx43). Cx43 is synthesized in the rough endoplasmic reticulum, transported to the Golgi apparatus, and ultimately trafficked to the plasma membrane (5, 6). Recent evidence has suggested that Cx43 is involved in modifying arrhythmogenic conditions (7, 8) since Cx43 knockout mice were subject to sudden death caused by lethal arrhythmia, including ventricular tachycardia, or fibrillation (9, 10). Although many other factors, including sodium, potassium, and calcium channels, appear to be involved in arrhythmogenicity, it is speculated that functional deletion of Cx43 is also responsible for arrhythmia. To date, it has remained unclear whether and how ACh modulates Cx43. Therefore, we focused on the effect of ACh on Cx43.

Materials and Methods

Cell culture and pharmacological agents

H9c2 cells, which are spontaneously immortalized ventricular myoblasts from rat embryos, were used due to their conserved electrical and signal transduction characteristics (11). The cells were cultured in DMEM supplemented with 10% FBS and antibiotics. H9c2 cells were pretreated with 1 mM ACh for 8 h, followed by 1 h of hypoxia (1% of oxygen concentration). We chose N^{ω}-nitro-L-arginine methyl ester (L-NAME) (Sigma Chemical Co., St Louis, MO, USA), a specific nitric oxide (NO) synthase inhibitor, to determine whether NO mediates the signal transduction for Cx43 expression. L-NAME (1 mM) was administered for 1 h together with ACh, followed by hypoxia for 1 h. H9c2 cells were also treated with 1 mM *S*-nitroso-*N*-acetyl-l,l-penicillamine (SNAP) (Sigma Chemical Co.) before hypoxia. We used 10 μM Cbz-leu-leu-leucinal (MG132) (Sigma Chemical Co.) or 1 μM okadaic acid to investigate whether hypoxia enhanced Cx43 degradation or phosphorylation was important for regulating the functional activity of Cx43.

Western blot analysis

Cells were harvested from the dishes and prepared for immunoblotting as described previously (8). After washing in PBS, cells were lysed with SDS sample buffer and boiled for 10 min. After electrophoresis in a 10% SDS-polyacrylamide gel, proteins were transferred to a polyvinylidene difluoride membrane. The membrane was soaked in 4% skim milk in TBST solution overnight, then incubated with an anti-Cx43 polyclonal antibody (ZYMED Laboratories, Inc., South San Francisco, CA, USA) for 1 h, thoroughly washed, and then incubated with an anti-rabbit IgG secondary antibody (BD Transduction Laboratories, San Diego, CA, USA) for 40 min. Finally, the membrane was washed and subjected to chemiluminescent detection using the ECL Plus Western Blotting Detection Reagents (Amersham Biosciences, Piscataway, NJ, USA). We performed repeatedly 3-5 times each experiment using duplicate samples. The Western blotting data were analyzed using Kodak 1D Image Analysis Software (Eastman Kodak Co., Rochester, NY, USA).

Immunohistochemistry

H9c2 cells were fixed with 4% paraformaldehyde for 10 min and permeabilized with 1% Triton X-100 for another 10 min. To block nonspecific antibody binding, cells were incubated with 5% skim milk and successively incubated with an anti-Cx43 polyclonal antibody (ZYMED Laboratories, Inc.), in 1% skim milk at 4°C overnight and then with a Cy3-labeled secondary antibody (Jackson ImmunoReserch Laboratories, West Grove, PA, USA) at 4°C overnight. Actin staining was performed using FITC-conjugated phalloidin and then examined with a laser scanning confocal microscope.

Functional analysis of gap junction using a scrape and scratch method

A scrape-loading method can be used to introduce macromolecules into cultured cells by inducing a transient tear in the plasma membrane without affecting cell viability, thereby allowing sensitive determination of cell-cell communication. Following the treatment with ACh or okadaic acid, cells cultured on a coverslip were rinsed with PBS, and then 1% Lucifer Yellow was applied to the center of the converslip. A 27 gauge needle was used to create two longitudinal scratches through the cell monolayer. The cells were incubated in the dye mix for exactly 1 min, quickly rinsed three times with PBS, and finally examined by fluorescence microscopy. Lucifer Yellow does not diffuse through intact plasma membranes, but its low molecular weight permits its transmission from one cell to another, presumably across patent gap junctions (12 – 16). The area of the dye transferred from the scratched margin in hypoxia or hypoxia with ACh treatment was semi-quantified using the NIH image system and compared with that in normoxia.

Statistical analyses

Data are presented as the mean ± S.E.M. Differences

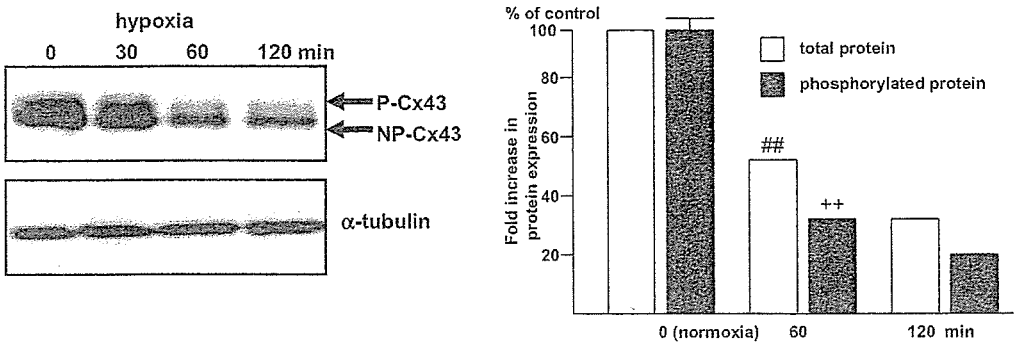

Fig. 1. Cx43 phosphorylation is decreased by hypoxia. Cells are subjected to 30 – 120 min of hypoxia and then analyzed by Western blot analysis. Cx43 phosphorylation (P-Cx43) is reduced to 32 ± 4% of the level under normoxia ($^{++}P<0.01$ *vs* 0 min, $^{\#\#}P<0.01$ *vs* 0 min) by 1% hypoxia, and the effect is remarkable after 60 min of hypoxia. NP-Cx43: non-phosphorylated form of Cx43. Open bars: total Cx43 protein level, closed bars: P-Cx43 level. Representative data from 5 independently performed experiments are shown (n = 5).

were assessed by ANOVA followed by Fisher's PLSD for multiple comparisons. The results were considered statistically significant at the level of $P<0.05$.

Results

Hypoxia decreases the Cx43 protein level in H9c2 cells

Several different forms of Cx43 were observed in the case of H9c2 cell (Fig. 1). The upper bands represented the phosphorylated forms, while the lower band corresponded to the non-phosphorylated form. We examined the acute effect of hypoxia on the total Cx43 protein level in H9c2 cells (n = 5). The total protein level of Cx43, including NP-Cx43 and P-Cx43, gradually decreased during hypoxia (Fig. 1), and 60 min of hypoxia induced a remarkable decrease in the total Cx43 protein level ($^{\#\#}P<0.01$ *vs* 0 min of hypoxia) and reduced its phosphorylation to 32 ± 4% of the normoxic level ($^{++}P<0.01$ *vs* 0 min of hypoxia). These results suggest that the total Cx43 protein level is rapidly decreased under hypoxia.

ACh increases the Cx43 protein level in H9c2 cells under normoxia or hypoxia

To determine whether ACh could modulate the Cx43 protein level after acute treatment, we initially treated H9c2 cells with 1 mM ACh under normoxia (n = 3). When the cells were stimulated with 1 mM ACh under normoxia, the Cx43 protein level was transiently increased ($^{++}P<0.01$ *vs* 0 min), followed by a rapid decrease, and then another peak was observed at 8 h (Fig. 2A). Next, to examine the effect of ACh on the hypoxia-induced decrease in Cx43, we pretreated H9c2 cells with 1 mM of ACh for 7 h, followed by 1 h of hypoxia (n = 6). Compared to the Cx43 level under hypoxia alone (hypoxia), the Cx43 protein level in ACh-pretreated H9c2 cells was not decreased under hypoxia (ACh + hypoxia), but instead was rather sustained ($^{\#\#}P<0.01$ *vs* hypoxia; ns, not significant *vs* normoxia; n = 6) (Fig. 2B). This ACh-mediated inhibition of the decrease in Cx43 under hypoxia was also observed by immunocytochemistry since hypoxia decreased the Cx43 immunoreactivity, and ACh inhibited the reduction (Fig. 2C).

Inhibition of the decrease in the Cx43 protein level during hypoxia by ACh occurs via NO

To further characterize the signal transduction for ACh-mediated inhibition of the reduction in the Cx43 protein level under hypoxia, we investigated the effects of chemicals on the Cx43 protein level (n = 5) (Fig. 3). Pretreatment with L-NAME (1 mM) for 1 h inhibited the ACh-induced recovery of the Cx43 protein level during hypoxia, suggesting that NO participates in regulating the Cx43 protein level ($^{\#}P<0.05$ *vs* ACh, n = 5). To further investigate whether the protein level was affected by NO, the cells were treated with 1 mM SNAP, a NO donor, instead of ACh. SNAP partially inhibited the reduction in the Cx43 protein level compared with L-NAME treatment, further suggesting that NO plays a partial role in modulating the protein level ($^{+}P<0.05$ *vs* L-NAME, n = 5).

Cx43 is degraded under hypoxia

To further investigate the mechanisms of the decrease in Cx43 under hypoxia, H9c2 cells were pretreated with the proteasome inhibitor MG132 (n = 5) for 10 and 60 min during hypoxia (Fig. 4A). The proteasome inhibition produced a striking recovery of the decreased total Cx43 protein level. MG132 inhibited the reduction

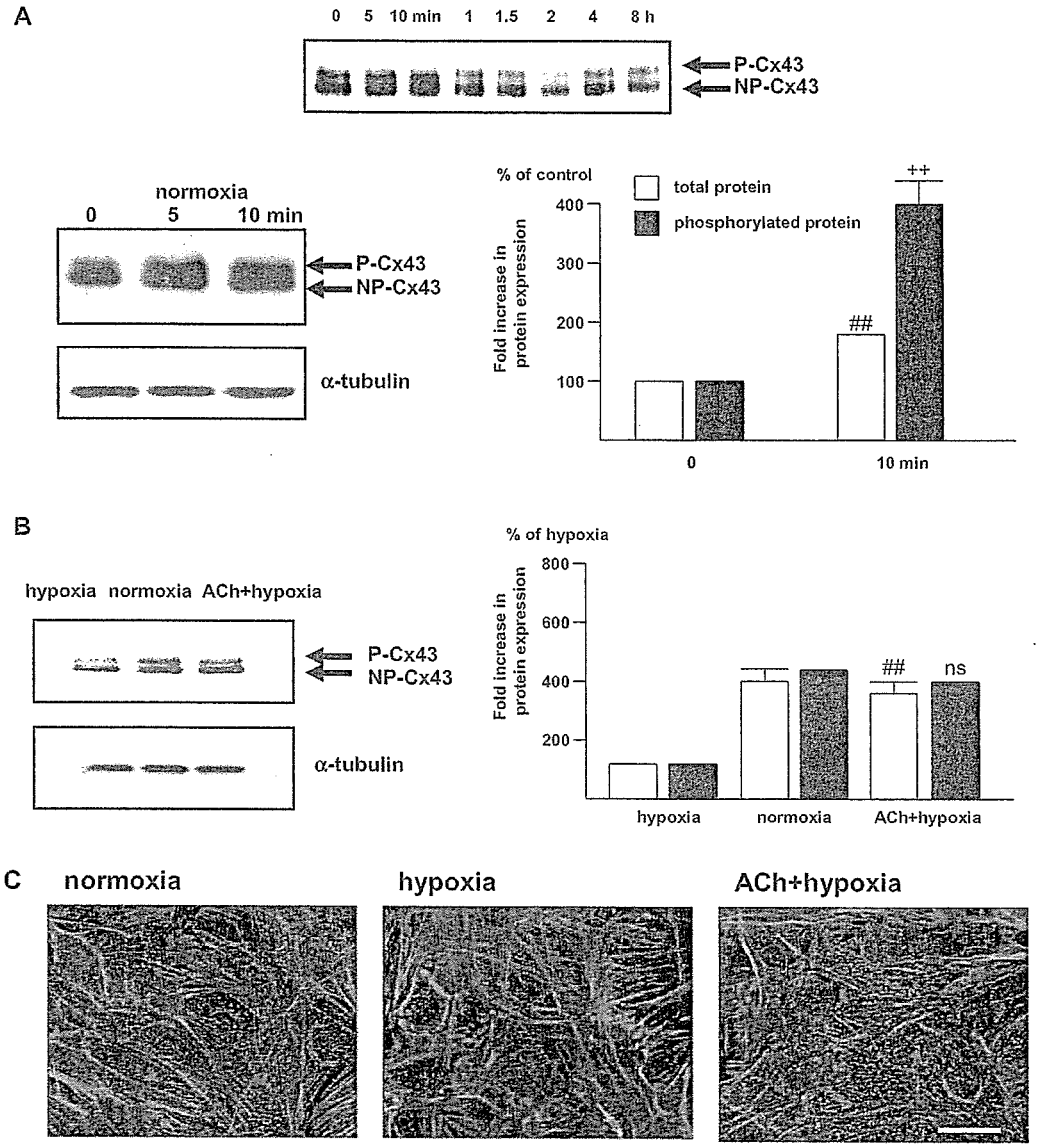

Fig. 2. ACh regulates Cx43 phosphorylation under normoxia and hypoxia. A: 1 mM ACh increases Cx43 phosphorylation (P-Cx43) in the acute phase under normoxia, reaching a peak of 409 ± 28% at 10 min ($^{++}P<0.01$ *vs* 0 min, $^{\#\#}P<0.01$ *vs* 0 min, n = 3). The entire time course shows another peak of the Cx43 protein level following the acute phase at 8 h. B: ACh suppresses the reduction in the Cx43 protein level induced by 1 h of hypoxia. ACh (1 mM) pretreated H9c2 cells show a sustained level of Cx43 phosphorylation, comparable to that under normoxia (normoxia), even under hypoxia (ACh + hypoxia) ($^{\#\#}P<0.01$ *vs* hypoxia; ns, not significant *vs* normoxia; n = 6). C: ACh inhibits the reduction in Cx43 immunoreactivity under hypoxia (red dots). Representative staining is shown. Cx43 is indicated by red dots. Bar: 50 μm.

in the Cx43 protein level by hypoxia for up to 60 min, suggesting that the reduction is due to activation of Cx43 protein degradation ($^{\#}P<0.05$ *vs* normoxia, n = 5). Furthermore, the effect of MG132 on inhibiting Cx43 degradation was not modified by ACh addition, and as a consequence, the effect of MG132 on inhibiting the hypoxia-induced decrease in Cx43 was comparable to that of cotreatment with MG132 and ACh (not significant *vs* ACh + MG132, n = 5) (Fig. 4B). These results suggest that ACh modulates the degradation process of Cx43.

ACh activates the function of gap junctions through an increase in the Cx43 protein level

To investigate whether ACh inhibition of the Cx43 protein level during hypoxia leads to functional recovery of gap junctions, we applied the scrape/scratch technique (n = 5). In a control experiment, scrape-loaded

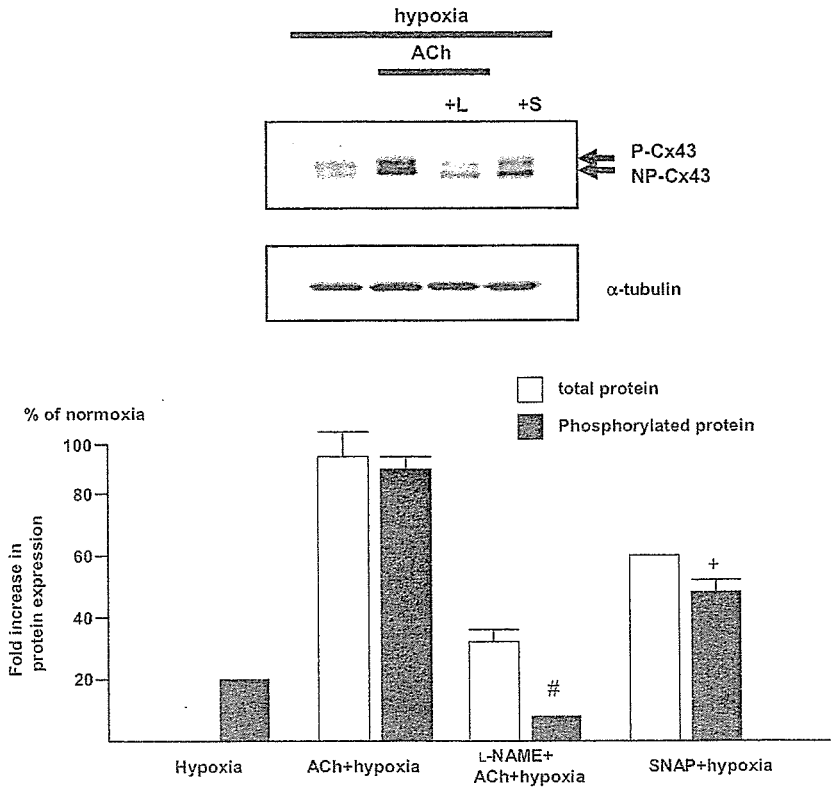

Fig. 3. NO is involved in the ACh signaling pathway that leads to the increase in Cx43 phosphorylation ($^{\#}P<0.05$ *vs* ACh + hypoxia; $^{+}P<0.05$ *vs* L-NAME + ACh + hypoxia). ACh: 1 mM ACh, L: 1 mM L-NAME, S: 1 mM SNAP. Representative data from 5 independently performed experiments are shown (n = 5).

cells in the presence of Lucifer Yellow showed positive transfer of Lucifer Yellow between cells. In contrast, cells treated with hypoxia appeared to lose their ability to communicate with each other and the dye transfer was blocked to 6 ± 2% of the intensity under normoxia. In contrast, ACh suppressed the hypoxia-induced blockage of dye transfer ($^{\#\#}P<0.01$ *vs* hypoxia, not significant *vs* normoxia, n = 5). The area of Lucifer Yellow fluorescence was increased in ACh-treated cells along the scraped margin during hypoxia (62 ± 10% of the area under normoxia) (Fig. 5). These results suggest that hypoxia affects intercellular communication and that ACh functionally activates cell-cell communication, even under hypoxia, through increases in the Cx43 protein level. Furthermore, pretreatment with 1 μM okadaic acid, a phosphatase inhibitor, for 10 min recovered the reduction in the Cx43 protein level and the extent of dye transfer during hypoxia (Fig. 6). Taken together with the results obtained with the proteasome and phosphatase inhibitors, it is suggested that both the protein and phosphorylation levels of Cx43 are involved in the function of Cx43.

Discussion

In the current study, we have shown that the Cx43 protein level is regulated by ACh in the presence or absence of hypoxia. Even in normoxia, ACh regulated the Cx43 protein level and inhibited the reduction in the Cx43 protein level induced under hypoxia. Such modification of the Cx43 protein level by ACh partially occurred via NO, since the protein level sustained by ACh during hypoxia was affected by L-NAME, whereas SNAP showed similar effects to ACh. Furthermore, the results indicated that the hypoxia-induced decrease in the total Cx43 protein level is due to proteasome degradation. Taken together, these results further suggest that ACh is involved in inhibiting Cx43 degradation under hypoxia.

Our previous study revealed that vagal stimulation inhibited the reduction in the Cx43 protein level during acute myocardial ischemia and instead sustained a similar level to that in the normal heart (4). As a result, vagal stimulation was further shown to decrease the frequency of ventricular arrhythmia. Moreover, ACh sustained the dye transfer level, which was attenuated